


Article

Integrated Modeling Approach to Assess Freshwater Inflow Impact on Coastal Water Quality

Shreeya Bhattarai ^{1,*}, Prem Parajuli ^{1,*}  and Anna Linhoss ²

¹ Department of Agricultural and Biological Engineering, Mississippi State University, Starkville, MS 39762, USA

² Department of Biosystems Engineering, Auburn University, Auburn, AL 36849, USA

* Correspondence: pparajuli@abe.msstate.edu

Abstract: The quality of freshwater input from tributaries of the Western Mississippi Sound (WMSS) impacts the quality of coastal water. Hydrological and hydrodynamic models can be coupled to assess the impact of freshwater inflow from coastal watersheds. This study aims to compare the performance of a hydrodynamic model and a hydrological–hydrodynamic coupled model in detecting the effect of freshwater inflow from the coastal watersheds of the state of Mississippi into the WMSS. A hydrological model, the Soil and Water Assessment Tool (SWAT), and a hydrodynamic model, the visual Environmental Fluid Dynamics Code (vEFDC), were coupled to evaluate the difference between the hydrodynamical modelling approach, which employs an area-weighted approach to define flow and nutrient concentrations, and the more recent coupling model approach, which uses a hydrological model to determine the flow and nutrient load of the model. Furthermore, a nutrient load sensitivity analysis of the effect of freshwater inflow on water quality in the WMSS was conducted in addition to assessing the repercussions of tropical depressions. Hydrological assessments of the major tributaries watersheds of Saint Louis Bay (SLB) at the WMSS were performed using the SWAT model. After calibration/validation of the SWAT model, the streamflow output from the SWAT was incorporated into the vEFDC model. Finally, hydrodynamic simulation of the SWAT-vEFDC model was conducted, and water quality output was compared at different SLB locations. The salinity, dissolved oxygen, total nitrogen (TN), and total phosphorus (TP) were assessed by comparing the vEFDC and SWAT-vEFDC outputs. The results indicated that hydrological input from the SWAT alters the flow and nutrient concentration results as compared to an area-weighted approach. In addition, a major impact on the concentration of TN and TP occurred at the location where the freshwater flows into SLB. This impact diminishes further away from the point of freshwater inflow. Moreover, a 25% nutrient load variation did not demonstrate a difference in water quality at the WMSS besides TN and TP in a post-tropical depression scenario. Therefore, the SWAT-vEFDC coupled approach provided insights into evaluation of the area-weighted method, and of hydrological model output to the hydrodynamical model, the effect of freshwater inflow into coastal waters, and nutrient sensitivity analysis, which are important for integrated coastal ecosystems management.

Keywords: coupling models; SWAT; vEFDC; water quality assessment; nutrient sensitivity; extreme weather



Citation: Bhattarai, S.; Parajuli, P.; Linhoss, A. Integrated Modeling Approach to Assess Freshwater Inflow Impact on Coastal Water Quality. *Water* **2024**, *16*, 3012. <https://doi.org/10.3390/w16213012>

Academic Editor: Qianqian Zhang

Received: 17 July 2024

Revised: 2 October 2024

Accepted: 10 October 2024

Published: 22 October 2024



Copyright: © 2024 by the authors. Licensee MDPI, Basel, Switzerland. This article is an open access article distributed under the terms and conditions of the Creative Commons Attribution (CC BY) license (<https://creativecommons.org/licenses/by/4.0/>).

1. Introduction

The unique environment present in aquatic ecosystems sustains diverse biodiversity and provides environmental benefits by preventing floods and serving as natural filters. Water quality assessment is essential for the sustainable management of aquatic ecosystems [1–3]. A comprehensive understanding of the source, transport, and fate of water contaminants is necessary to develop site-specific management strategies. Numerical modelling techniques offer time- and cost-effective measures to investigate hydrological

dynamics under different scales and circumstances [4–9]. Approaches that integrate watershed and receiving water models have gained popularity due to their effective application in understanding water quality hydrodynamics [10–14]. Watershed models simulate hydrology using geomorphologic, land use, and meteorological data and can assess water quality [15]. Receiving water models are implemented in waterbodies, such as large rivers, reservoirs, wetlands, and estuaries, which receive water from the upstream watershed to simulate the hydrodynamics and water quality interactions within the waterbody. Bathymetric, meteorological, hydrological, and water quality data are required for modelling hydrodynamics and water quality in receiving waters [16,17]. Boundary conditions, such as inflow, outflow, tides, winds, water levels, and water quality, define the physical conditions at the boundary and are vital for achieving accurate model outputs [16,17]. Thus, watershed models can provide simulated flow and water quality data for upstream tributaries that lack continuously recorded data.

This study focused on the hydrodynamic and water quality assessment of the Western Mississippi Sound (WMSS), Gulf of Mexico. The WMSS water is designated for shellfish harvesting and recreational activities [18] and thus, water quality is a vital issue. The major sources of freshwater input into the WMSS are the Pearl River, the Jourdan River, the Wolf River, the Bonnet Carré Spillway, and several other smaller streams and bayous including Johnson Bayou, Bayou Portage, Four Dollar Bayou, and Rotten Bayou. In the past, the hydrodynamic model of the WMSS was developed and linked with the hydrodynamic model for the Lower Pearl River (LPR) using the visual Environmental Fluid Dynamic Code (vEFDC) [19,20] tool. In the linked model, the output of the LPR model was input into the WMSS grid, henceforth called the WMSS-LPR_vEFDC model, which represented the riverine flow, estuarine circulation and simulated flow, surface water elevation, temperature, and salinity [19]. The author suggested that the linked WMSS-LPR_vEFDC model was able to be integrated with the water quality and habitat suitability model to study the impact of hydrological variability. Later, the WMSS water quality model, henceforth called the vEFDC model, was developed by Bazgirkhoob et al. [21] to simulate dissolved oxygen at different vertical strata and with the changing seasons. Here, the WMSS-LPR_vEFDC model developed by Armandei et al. [19] was used in conjunction with the water quality model CE-QUAL-ICM to build the vEFDC model. This hydrodynamic water quality model was verified and validated for nitrogen, phosphorus, and chlorophyll-a [21]. Since measured water quality data from the Wolf River and the Jourdan River were unavailable, simulated water quality concentration data from the LPR model were used as inputs for these smaller rivers. It is likely that differences in geomorphology and land use in the smaller rivers compared to the Pearl River lead to differences in water quality flowing out of these rivers. Therefore, to address the research gap in previous studies, where an area-weighted approach was used to determine the flow and nutrient concentration of the Wolf River watershed and the Jourdan River watershed from the proximately located Pearl River watershed model, this study aims to incorporate SWAT model flow and nutrient data from the Wolf River and the Jourdan River into the vEFDC model to evaluate the water quality at various locations within WMSS. For this purpose, the coupled hydrological and hydrodynamic models in the present study are henceforth called the SWAT-vEFDC model. The major objective of this study is to compare the output of the vEFDC model developed with an area-weighted approach and the SWAT_vEFDC coupled model to see the variation in the simulated flow and water quality parameters. Moreover, this study assesses the impact of freshwater flows from the coastal watersheds of Mississippi into the WMSS by coupling the SWAT and vEFDC models. This study focuses on coupling two watershed models of the Wolf River and the Jourdan River with the vEFDC model to make a composite river–bay–estuary modelling system for assessing the effect of freshwater introduction on the water quality at various locations in SLB and the WMSS. This study builds upon a previous water quality assessment where the dissolved oxygen level was analyzed throughout the WMSS considering the calculated freshwater inflow and water quality concentration from the Wolf River and the Jourdan River on the basis of the weighted

average method obtained from the Pear River model [21]. The findings of this study indicated that a satisfactory trend and correlation between the area-weighted method flow and hydrologically simulated flow was observed. Varying concentrations of total nitrogen (TN) and total phosphorus (TP) were observed at the freshwater inflow area, but were later minimized while moving further towards the WMSS.

2. Materials and Methods

2.1. Study Area

The location of the study area is shown in Figure 1a–c, illustrating the WMSS, the Jourdan River watershed (JRW), the Wolf River watershed (WRW), and their respective locations in the state of Mississippi, USA. The WMSS is a semi-enclosed estuary in the northern Gulf of Mexico which has a total surface area of 2255 km² [21]. It is bounded to the east by the Mississippi and Louisiana coastlines, including the city of Gulfport; to the south by Ship Island, Cat Island, and the Biloxi Marsh; and to the west by Lake Borgne. The Jourdan River and the Wolf River are the major sources of freshwater input, draining into the SLB of the WMSS. Forestry land use dominates the JRW, whose estimated area is 538 km². The land use in JRW consists of 37.9% evergreen forest, 26.6% rangeland, 18.26% pasture, and 17.3% forested wetlands. Likewise, WRW is also a forest-dominated watershed. The WRW area is estimated to be 801 km², of which 7.7% is pasture, 20.8% is forested wetland areas, 24.9% is range-brush areas, and 46.6% is evergreen forests [22]. The WMSS is designated for shellfish harvesting and recreational activities [18], which aid Mississippi's economy.

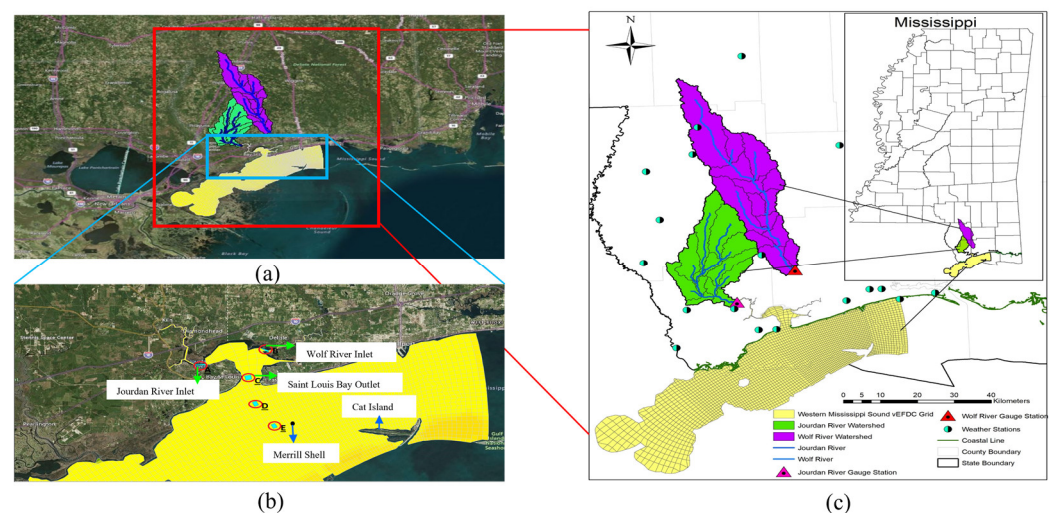


Figure 1. (a) Wider view of the Western Mississippi Sound showing the vEFDC grid in yellow, the SWAT-delineated upstream Jourdan River watershed in green, and the Wolf River watershed in violet. (b) Image showing water quality assessment cell in the Western Mississippi grid at locations A, B, C, D, and E. (c) Map of the study area showing the Wolf River watershed, the Jourdan River watershed, and the Western Mississippi Sound grid in the state of Mississippi.

2.2. Description of SWAT and EFDC Models and Their Coupling Process

The SWAT [23] is a comprehensive hydrological model which is used to simulate and predict the impact of land management practices and climate change on water quantity and water quality [24]. It is a watershed scale model used in different topographies to simulate a wide range of environmental processes including surface runoff, groundwater flow, erosion, nutrient transport, and crop yield [22,24–27]. The basic input data required to set up, calibrate, and validate the SWAT model are elevation, land use, land cover, soil, climate, management practices, and continuous timestep stream flow data. The SWAT model has been widely used in recent studies for watershed management, climate change assessment, nutrient management, integrated water resource management, and ecosystem services

such as carbon sequestration, with basic data and detailed objective-specific data [27–30]. This mathematical model divides the watershed into networks of subbasins that are further divided into unique hydrologic response units (HRUs) based on land use, soil type, and slope class [15]. The model simulates water balance and nutrient movement throughout the watershed.

In this study, the SWAT model setup was carried out by collecting site-specific elevation, land use, soil, climate, and streamflow data as listed in Table 1. Two separate models were set up for the JRW and the WRW. The JRW was divided into 13 subbasins with 233 HRUs and the WRW was divided into 15 subbasins with 489 HRUs. Both models were calibrated and validated according to the parameters listed in Bhattarai et al. [22] using the autocalibration tool SWAT Calibration and Uncertainty Program with Sequential Uncertainty Fitting version 2 (SWAT-CUP SUFI-2) [31]. The JRW was calibrated on a daily timestep from 10 March 2002 to 31 December 2003 and validated from 1 January 2004 to 30 September 2004, utilizing all the observed data available from the single gauge station USGS 02481660 at the JRW. In addition, the WRW was calibrated from January 1997 to December 2003 and validated from January 2004 to December 2010 on a monthly timestep, using the data collected from the USGS 02481510 gauge station. After adjusting the different parameters of both models, acceptable statistical values for comparing the observed and simulated flows were attained. The flowchart in Figure 2 illustrates the process of the SWAT model setup, calibration, and validation. Finally, the simulated streamflow from the calibrated/validated SWAT model was incorporated into the vEFDC model to study the impact of freshwater inflow into the coastal water.

Table 1. Basic data and their corresponding sources for the SWAT model setup.

S. No.	Data	Source
1	Elevation Data: Digital Elevation Model (DEM) (30 m × 30 m) (2020)	United States Geological Survey (USGS) (https://apps.nationalmap.gov/viewer/) (accessed on 4 October 2022)
2	Land-use and Land-cover Data: Cropland Data Layer (CDL) (2010)	United States Department of Agriculture-National Agricultural Statistics Service (USDA-NASS) (https://nassgeodata.gmu.edu/CropScape/) (accessed on 4 October 2022)
3	Soil Data: USSURGO (2020)	United States Soil Survey Geographic Database (US-SSURGO) SWAT-USSURGO (https://swat.tamu.edu/data/) (accessed on 4 October 2022)
4	Weather Data: NOAA (1995–2010) Precipitation, Maximum Temperature, Minimum Temperature	National Oceanic and Atmospheric Administration (NOAA) SWAT—Climate Data (https://swat.tamu.edu/data/) (accessed on 4 October 2022)
5	Discharge Data: -USGS 02481660 (2002–2005) (Jourdan River Nr Bay St Louis) -USGS 02481510 (1997–2010) (Wolf River Nr Landon)	United States Geological Survey (USGS) (https://waterdata.usgs.gov/ms/nwis/) (accessed on 5 October 2022)

The EFDC [16,17] is a state-of-the-art hydrodynamical modelling tool used to predict water quality and anthropogenic impacts on rivers, estuaries, lakes and reservoirs, wetlands, and coastal areas. The EFDC can use a three-dimensional hydrodynamic module to simulate the movement and mixing of water and contaminants in the water column and assess the sediment and nutrient transport and fate [16,17]. The EFDC is a numerical modelling tool that can simulate a wide variety of physical and biological phenomena, such as temperature, salinity gradient, dissolved oxygen (DO) level, nutrient load, growth, and decay of phytoplankton. The vEFDC [20] is a graphical user interface of the EFDC tool which offers a convenient way to create meshes, set up and run EFDC simulations, and visualize and analyze outputs. This is a multifunctional tool that can be coupled with watershed models to provide a more comprehensive analysis of the water body [19,21].

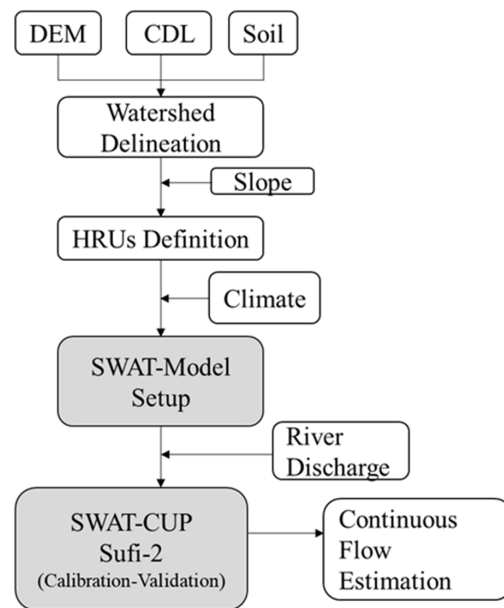


Figure 2. Flowchart of the SWAT model setup. (DEM: Digital Elevation Model, CDL: Cropland Data Layer, HRU: Hydrologic Response Units, SWAT-CUP Sufi-2: SWAT Calibration and Uncertainty Programs with Sequential Uncertainty Fitting version 2).

Using the vEFDC tool, an integrated 3D hydrodynamic model of the WMSS and the LPR was developed and calibrated by Armandei et al. [19], but it was not used for the simulation of water quality. Later, Bazgirkhoob et al. [21] assessed DO level, seasonality, and vertical stratification by integrating the vEFDC model and a water quality model named CE-QUAL-ICM. In the present study, the calibrated/validated flow from the SWAT model simulation of the JRW and the WRW are incorporated into the qser.inp file of the vEFDC model to couple the vEFDC model and the SWAT model to assess the impact of freshwater inflow on the concentration of DO, salinity, TN, and TP at different locations in the SLB and the WMSS. Figure 3 illustrates the flowchart of the SWAT-vEFDC coupling process:

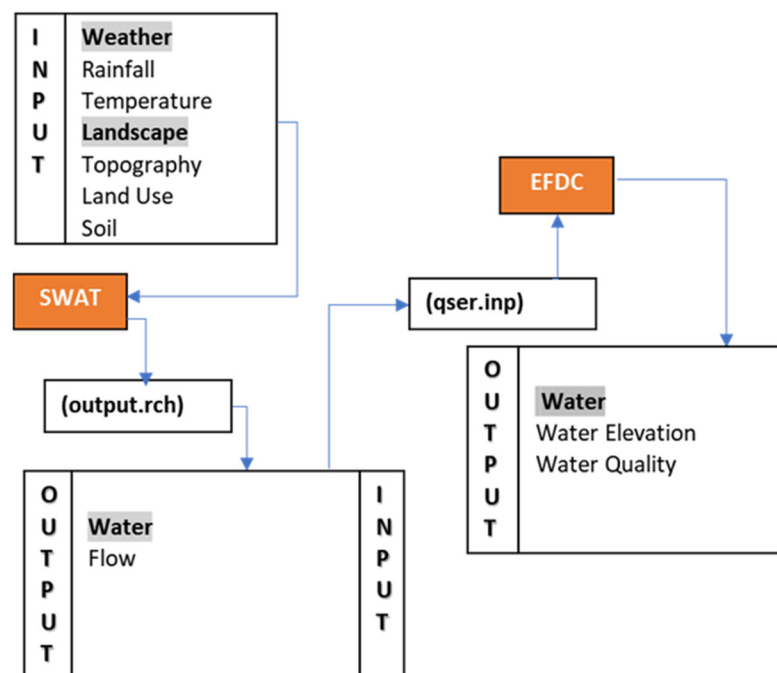


Figure 3. Schematic diagram of the SWAT-vEFDC model coupling process.

2.3. Water Quality Parameters

Salinity is the amount of dissolved salt in water. Salinity levels vary widely between freshwater, where it measures less than 1000 ppm, and coastal water, where it can exceed 35,000 ppm [32]. Climatic factors and anthropogenic activities can greatly alter salinity [33]. In the EFDC, salinity serves as a hydrodynamic parameter that affects the buoyancy and mixing of water. It can also be used as a conservative tracer that verifies the transport process of the model and assists in the analysis of mass conservation. Salinity is essential for estuarine aquatic life. Additionally, salinity affects the chemical processes [34] influencing the transportation and fate of contaminants in aquatic systems.

Dissolved oxygen (DO) is a critical parameter of aquatic ecosystems, referring to the amount of oxygen dissolved in the water that is available for the survival of aquatic life and for various biogeochemical functions. The amount of dissolved oxygen in a water body affects the way nutrients move through the aquatic ecosystem [35]. It is a major component of water quality models, such as the EFDC, and it is important to monitor and manage DO levels when managing water quality. Nitrogen and phosphorus are critical nutrients [36] in aquatic ecosystems as their availability can limit the growth and production of primary producers. Thus, monitoring TN and TP levels is essential for water quality management [37]. In this assessment, the spatial analysis of the TN and TP parameters in filtered (Filt) and unfiltered (Unfilt) states was also observed. Total nitrogen (TN) refers to the sum of organic nitrogen, ammonia (NH₄), nitrate (NO₃), and nitrite (NO₂). In the vEFDC, TN is simulated as five state variables: three in organic forms (refractory particulate, liable particulate, and dissolved) and two in inorganic forms (ammonium and nitrate) [16,17]. In the model, the nitrate state variable represents the total of nitrate and nitrite.

TN = Dissolved inorganic nitrogen (DIN) + Dissolved organic nitrogen (DON) + Particulate organic nitrogen (PON)

i.e.,

TN = [Nitrate + Nitrite + Ammonia] + [Dissolved organic nitrogen] + [Refractory particulate organic nitrogen (RPON) + Labile particulate organic nitrogen (LPON)]

Therefore,

TN Filt = Dissolved inorganic nitrogen (DIN) + Dissolved organic nitrogen (DON)

TN Unfilt = Dissolved inorganic nitrogen (DIN) + Dissolved organic nitrogen (DON) + Particulate organic nitrogen (PON)

Total phosphorus (TP) refers to the sum of dissolved and particulate phosphorus. In vEFDC, TP is simulated as four state variables: three in organic forms (refractory particulate, liable particulate, and dissolved) and one in an inorganic form (dissolved and particulate phosphate) [16,17].

TP = Dissolved inorganic phosphorus (DIP) + Dissolved organic phosphorus (DOP) + Particulate organic phosphorus (POP)

i.e.,

TP = [Total orthophosphate (PO₄)] + [Dissolved organic phosphorus (DOP)] + [Refractory particulate organic phosphorus (RPOP) + Labile particulate organic phosphorus (LPOP)]

Therefore,

TP Filt = Dissolved inorganic phosphorus (DIP) + Dissolved organic phosphorus (DOP)

$$\text{TP Unfilt} = \text{Dissolved inorganic phosphorus (DIP)} + \text{Dissolved organic phosphorus (DOP)} + \text{Particulate organic phosphorus (POP)}$$

3. Results

3.1. Flow Assessment: Calibration and Validation

The statistical measures used to calibrate/validate flow and assess the accuracy of the SWAT model included the coefficient of determination (R^2), the Nash–Sutcliffe efficiency (NSE), percentage bias (PBAIS), and the Kling–Gupta efficiency (KGE). The KGE was defined as the objective function in the SWAT-CUP. In the JRW, the R^2 varied from 0.59 to 0.72, the NSE varied from 0.42 to 0.71, the PBAIS varied from 36.7 to 4.7, and the KGE varied from 0.55 to 0.68, for daily flow. Since the KGE was defined as the objective function, it indicated intermediate performance of the JRW model during calibration and validation, which was in the acceptable range. In the WRW, the R^2 varied from 0.82 to 0.75, the NSE varied from 0.81 to 0.73, the PBAIS varied from -4.9 to -3 , and the KGE varied from 0.80 to 0.70, for monthly flow. These results also indicated an acceptable performance of the SWAT model during calibration and validation [22,25,38]. For the calibration and validation of the vEFDC model, measured DO data were compared across the simulated data and achieved good statistics in terms of root mean square error, bias and R^2 at 11 different locations throughout the WMSS grid [21].

The graphs in Figure 4 show the comparison of the flow data used in the vEFDC model obtained using area-weighted measurement and the SWAT-vEFDC model simulated using a hydrological modelling tool for the Wolf River and the Jourdan River. Time series analysis of these two flow trends showed higher peaks in the area-weighted flow series. Statistical metrics demonstrated $R^2 = 0.66$ and $\text{NSE} = 0.61$ for the Wolf River flow; and $R^2 = 0.80$ and $\text{NSE} = 0.66$ for the Jourdan River. These results signify high goodness of fit for the two datasets.

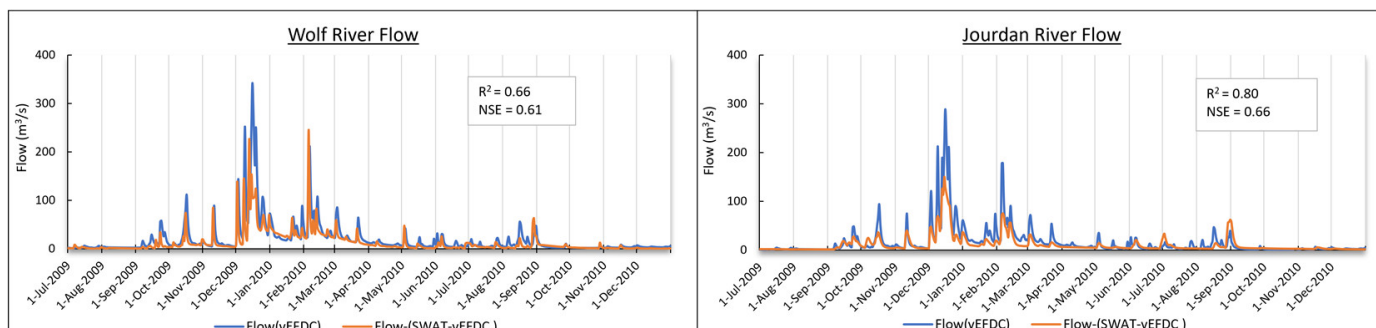


Figure 4. Flow comparison between the vEFDC model and the SWAT-vEFDC model.

3.2. Water Quality Assessment

The SWAT and vEFDC models were coupled and run from 1 January 2009 to 31 December 2010, skipping the first six months as a warmup period. The temporal variation in the concentration of DO, salinity, TN, and TP as simulated by the vEFDC model and the SWAT-vEFDC coupled model were compared at different locations, as presented in Figure 5a–e. Five locations, namely A, B, C, D, and E, as shown in Figure 1b, were selected to compare the vEFDC and SWAT-vEFDC simulation outputs. Location A (cell I = 62, J = 37, K = 4) is the Jourdan River inlet, location B (cell I = 68, J = 38, K = 4) is the Wolf River inlet, location C (cell I = 66, J = 31, K = 4) is where SLB opens up to the WMSS (approx. radial distance 7 km away from location A and 6 km away from location B), location D (cell I = 65, J = 25, K = 4) is in between the outlet of Saint Louis Bay and Merrill Shell (approx. radial distance 11 km away from location A and 12 km away from location B) and location E (cell I = 66, J = 16, K = 4) lies near Merrill Shell on the WMSS (approx. radial distance 16 km away from location A and 15 km away from location B). The statistical results obtained by

comparing the results of the vEFDC and SWAT-vEFDC models are presented in Table 2. The influence of the SWAT-vEFDC model outflow was observed for salinity, dissolved oxygen, and nutrients in the Jourdan inlet (A), the Wolf inlet (B) and the SLB outlet (C) while, in contrast, there was minimal distinction between the models' outputs at location D and location E.

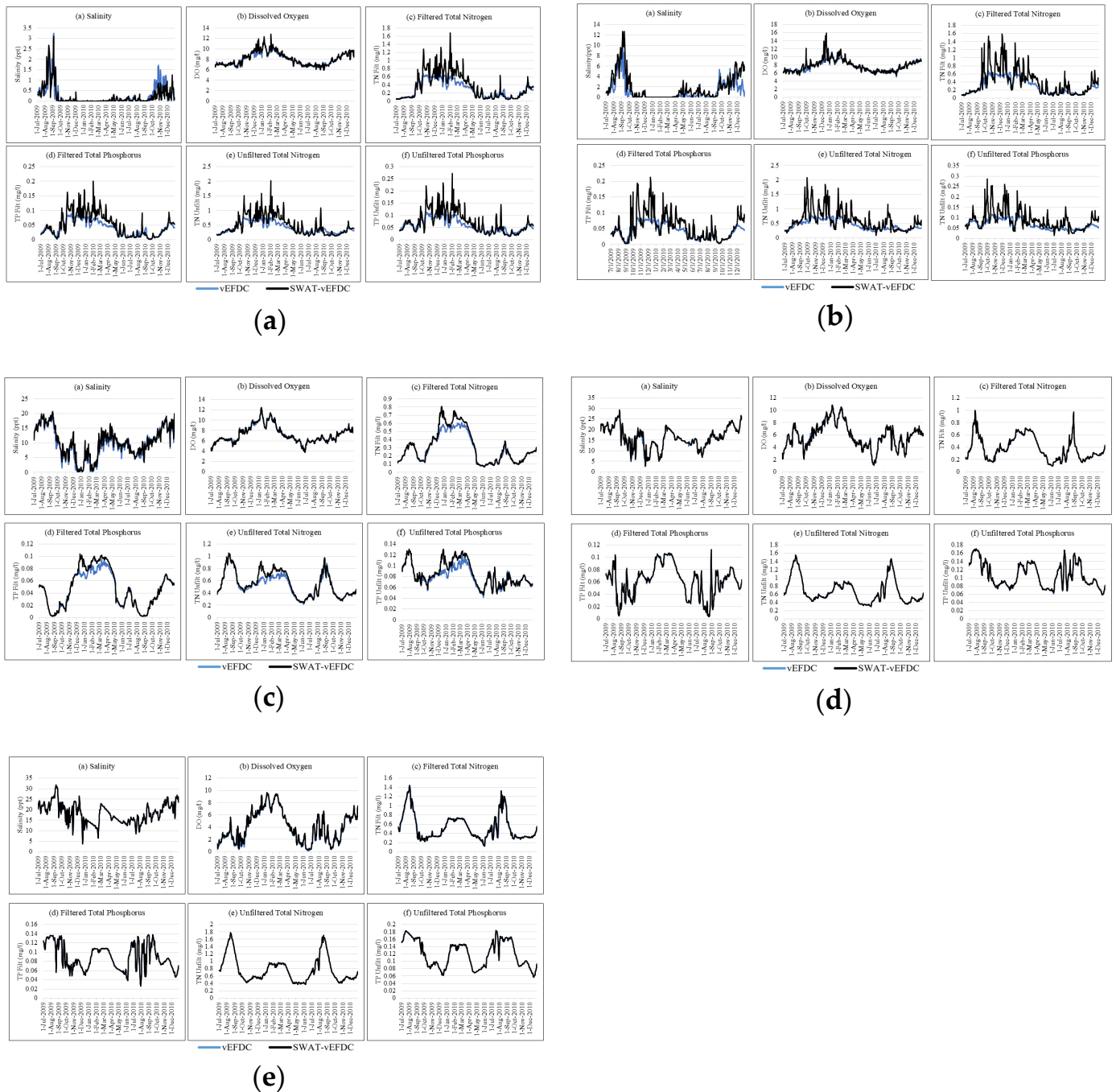


Figure 5. Temporal variation of salinity, dissolved oxygen, filtered total nitrogen, filtered total phosphorus, unfiltered total nitrogen, and unfiltered total phosphorus at the inlet of the Jourdan River at (a) location A, (b) location B, (c) location C, (d) location D and (e) location E. In (d,e), the vEFDC graph and the SWAT-vEFDC graph are overlapped.

Table 2. Summary of the statistical comparison between the vEFDC and SWAT-vEFDC models.

Location	Salt		DO		TN Filt		TP Filt		TN Unfilt		TP Unfilt	
	R ²	NSE	R ²	NSE	R ²	NSE	R ²	NSE	R ²	NSE	R ²	NSE
A	0.83	0.83	0.92	0.88	0.84	0.32	0.82	0.23	0.76	−0.3	0.75	−0.3
B	0.76	0.39	0.76	0.57	0.75	−0.35	0.71	−0.6	0.54	−2.4	0.50	−2.3
C	0.98	0.97	1	1	0.97	0.9	0.97	0.93	0.94	0.9	0.89	0.76
D	0.99	0.99	1	1	1	1	0.99	0.99	1	1	1	1
E	0.99	0.99	0.99	0.98	0.98	0.98	1	1	1	1	1	1

Increased differences were observed in the water quality parameters, especially TN Filt, TP Filt, TN Unfilt, and TP Unfilt, along the transects where freshwater flows into SLB, as shown in Figure 6. The graphs in Figure 6 compare the average daily concentration from 1 July 2009 to 31 December 2010 of the vEFDC and SWAT-vEFDC models plotted together.

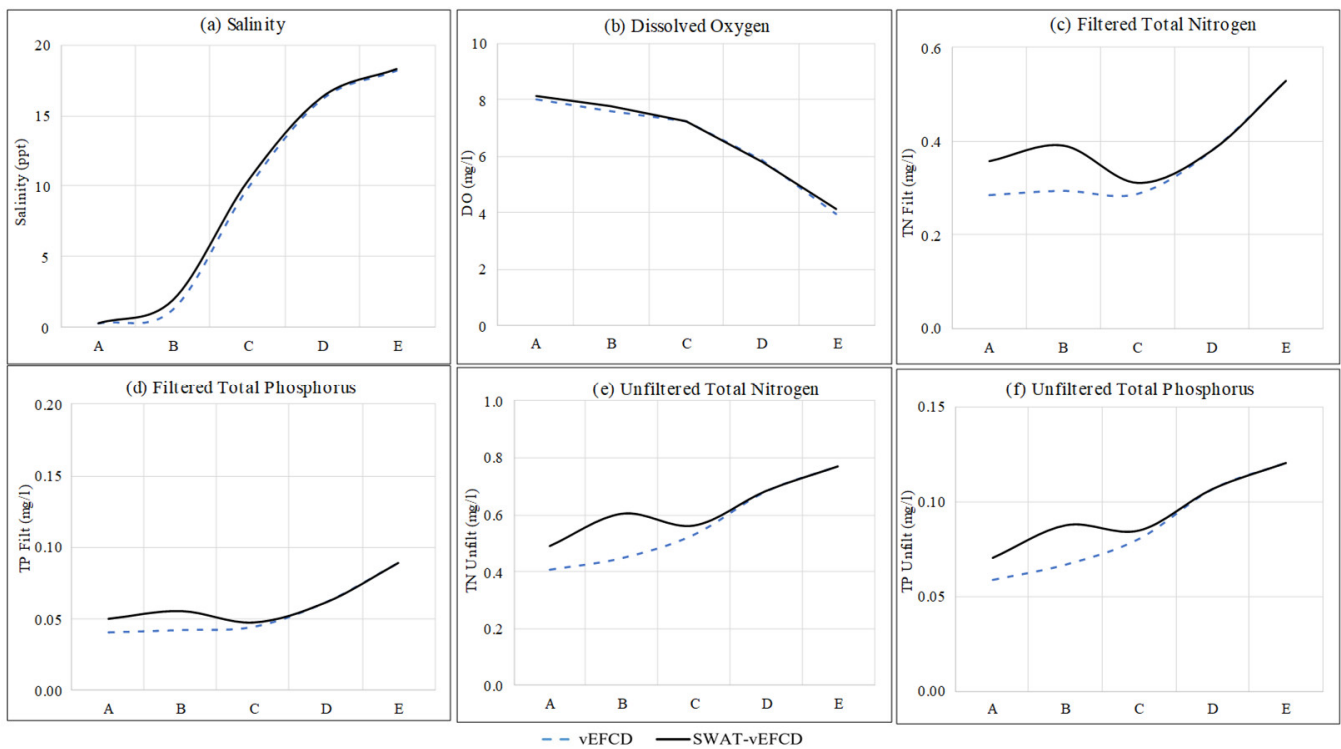


Figure 6. Average daily concentration of (a) salinity, (b) dissolved oxygen, (c) filtered total nitrogen, (d) filtered total phosphorus, (e) unfiltered total nitrogen, and (f) unfiltered total phosphorus from 1 July 2009 to 31 December 2010 simulated by the vEFDC and SWAT-vEFDC models at locations A, B, C, D, and E.

The box plot in Figure 7a–f shows the distribution of the concentration of DO, salinity, TN Filt, TP Filt, TN Unfilt and TP Unfilt at different locations. These plots are discussed individually in the following sections.

Salinity: Statistically comparing the performance of both models in terms of salinity, R² = 0.83 and NSE = 0.83 for location A. The average salinity concentration was 0.25 ppt in the vEFDC model and 0.23 ppt in the SWAT-vEFDC model. Similarly, for location B, R² = 0.76 and NSE = 0.39. Here, the concentration of salinity changed from 1.23 ppt to 1.88 ppt between the vEFDC and SWAT-vEFDC models. At location C, where R² = 0.98 and NSE = 0.97, the average daily simulated salinity concentration increased from 9.83 ppt in the vEFDC model to 10.27 ppt in the SWAT- vEFDC model. At location D, the results obtained were 0.99 for both R² and NSE. Here, the daily average salinity concentration

changed from 16.19 ppt to 16.26 ppt. Further down, at location E, the average daily salinity was 18.24 ppt in both the models, resulting in a 0.99 R^2 and 0.99 NSE. Both models showed lower salinity near the river outlets and higher salinity further away from the river outlets and toward the models' southern boundary. The concentration of salinity was the highest at location E. This shows that differences in the estimation of salinity concentration resulted from the two models.

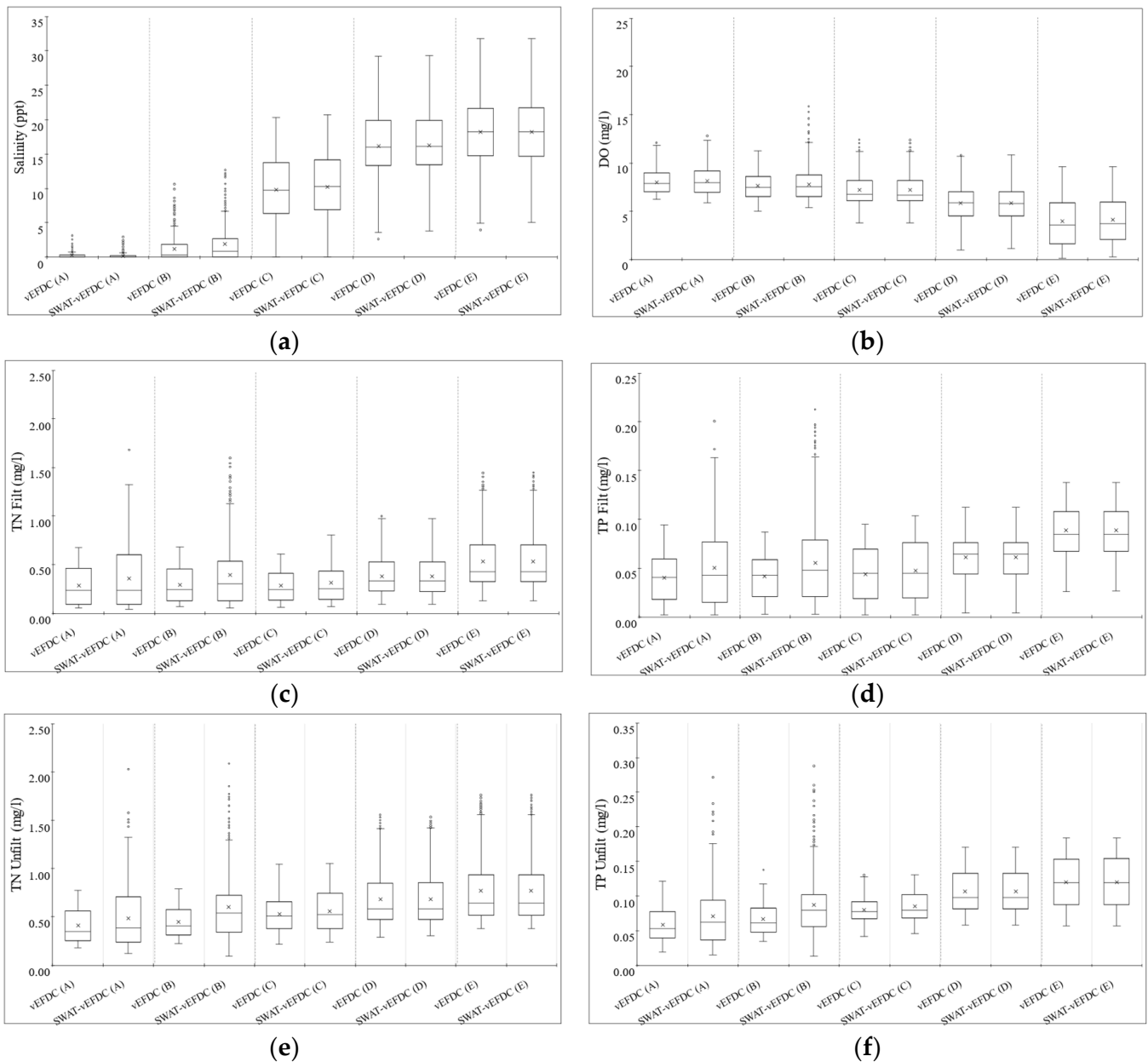


Figure 7. Distribution of (a) salinity, (b) dissolved oxygen (DO), (c) filtered total nitrogen, (d) filtered total phosphorus, (e) unfiltered total nitrogen and (f) unfiltered total phosphorus simulated by the vEFDC and SWAT-vEFDC models at locations A, B, C, D, and E across the Western Mississippi Sound.

Dissolved oxygen: Evaluating the performance of both models with respect to DO, $R^2 = 0.92$ and $NSE = 0.88$ were obtained for location A, with an average DO level increasing from 8.01 mg/L to 8.12 mg/L. At location B, the average daily DO was $R^2 = 0.76$ and $NSE = 0.57$, with the DO level changing from 7.62 mg/L to 7.81 mg/L. At location C, the average daily DO was $R^2 = 1.00$ and $NSE = 1.00$, with the DO level decreasing from 7.24 mg/L to 7.22 mg/L. At location D, R^2 and NSE were both 1.00, with the DO level

changing from 5.85 mg/L to 5.84 mg/L. At location E, the average daily DO was $R^2 = 0.99$ and $NSE = 0.98$, with the DO level increasing from 3.95 mg/L to 4.12 mg/L. The trends of simulated DO from both the models show that DO was highest at location A and location B, which are freshwater inlets. DO at location C was 7.24 mg/L and 7.22 mg/L as simulated by the vEFDC model and the SWAT-EFDC models, respectively. The DO decreased as it moved along the Western Mississippi sound near Merrill Shell, and was observed to be lowest at location E. These results demonstrate that the SWAT-vEFDC model estimated an increased difference in DO compared to that estimated by the vEFDC model.

TN Filt: Assessing vEFDC and SWAT-vEFDC model performance at estimating TN Filt, $R^2 = 0.84$ and $NSE = 0.32$ results were obtained for location A, with the average TN Filt level increasing from 0.28 mg/L to 0.36 mg/L. At location B, the average daily TN Filt was $R^2 = 0.75$ and $NSE = -0.35$, with the TN Filt level changing from 0.29 mg/L to 0.39 mg/L. At location C, the average daily TN Filt was $R^2 = 0.97$ and $NSE = 0.90$, with the TN Filt level changing from 0.29 mg/L to 0.31 mg/L. At location D, R^2 and NSE were both 1.00, with the TN Filt level remaining unchanged at 0.38 mg/L. At location E, R^2 and NSE were both 0.98, with the TN Filt level remaining constant at 0.53 mg/L. The trends of simulated TN Filt show that TN Filt was low at location A and location B, which are freshwater inlets. TN Filt level at location C was 0.29 mg/L and 0.31 mg/L as simulated by the vEFDC model and the SWAT-vEFDC integrated models, respectively. The TN Filt level increased nearer to Merrill Shell and was observed to be highest at location E. These results demonstrated that there were increases difference between the concentrations of TN Filt estimated by the vEFDC model alone and by the SWAT-vEFDC model.

TP Filt: Similarly, comparing the TP Filt obtained from the vEFDC model and the SWAT-vEFDC model, $R^2 = 0.82$ and $NSE = 0.23$ results were obtained at location A, with the average TP Filt level increasing from 0.04 mg/L to 0 mg/L. At location B, $R^2 = 0.71$ and $NSE = -0.56$, with the TP Filt level changing from 0.04 mg/L to 0.06 mg/L. At location C, $R^2 = 0.97$ and $NSE = 0.93$, with the TP Filt level changing from 0.04 mg/L to 0.05 mg/L. At Location d, R^2 and NSE were both 0.999, with the TP Filt level remaining unchanged at 0.06 mg/L. At location E, R^2 and NSE were both 1, with the TP Filt level being constant at 0.09 mg/L. The trends of simulated TP Filt level showed that TP Filt was low at location A, location B, and location C. TP Filt level at location C was 0.04 mg/L and 0.05 mg/L as simulated by the vEFDC model and the SWAT-vEFDC models, respectively. The TP Filt level increased nearer to Merrill Shell and was observed to be highest at location E. Again, these results demonstrated that there were increased differences between the estimation of TP Filt from the vEFDC model and the SWAT-vEFDC model.

TN Unfilt: Likewise, comparing the performance of TN Unfilt between the vEFDC model and the SWAT-vEFDC model, $R^2 = 0.76$ and $NSE = -0.25$ results were obtained at location A, with the average TN Unfilt level increasing from 0.41 mg/L to 0.49 mg/L. At location B, $R^2 = 0.54$ and $NSE = -2.37$, with the TN Unfilt level changing from 0.45 mg/L to 0.60 mg/L. At location C, $R^2 = 0.94$ and $NSE = 0.89$, with the TN Unfilt level increasing from 0.53 mg/L to 0.56 mg/L. At location D, R^2 and NSE were both 1.00, with the TN Unfilt level remaining constant at 0.68 mg/L. Similarly, at location E, the average daily R^2 and NSE were both 1.00, with the TN Unfilt remaining unchanged at 0.77 mg/L. The trends of simulated TN Unfilt show that TN Unfilt was lower at locations A, B, and C as compared to locations D and E. The TN Unfilt level at location C was 0.53 mg/L and 0.56 mg/L as simulated by the vEFDC model and the SWAT-vEFDC models, respectively. The TN Unfilt level increased as it moved along the Western Mississippi Sound near Merrill Shell, and was observed to be highest at location E. These results demonstrate considerable difference between the estimation of TN Unfilt from the vEFDC model and the SWAT-vEFDC model.

TP Unfilt: Evaluating model performance for TP Unfilt between the vEFDC model and the SWAT-vEFDC model, $R^2 = 0.75$ and $NSE = -0.26$ results were obtained at location A, with the average TP Unfilt level increasing from 0.06 mg/L to 0.07 mg/L. At location B, $R^2 = 0.50$ and $NSE = -2.26$, with the TP Unfilt level increasing from 0.07 mg/L to 0.09 mg/L. At location C, $R^2 = 0.89$ and $NSE = 0.76$, with the TP Unfilt level remaining constant at

0.08 mg/L. At location D, R^2 and NSE were both 1.00, with the TP Unfilt level remaining constant at 0.11 mg/L. Likewise, at location E, R^2 and NSE were both 1.00, with the TP Unfilt level remaining constant at 0.12 mg/L. The trends of simulated TP Unfilt show that TP Unfilt was lowest at locations A, B, and C. The TP Unfilt level at location C remained constant at 0.008 mg/L as simulated by both the vEFDC model and the SWAT-vEFDC coupled model. The TP Unfilt level increased as it moved along the Western Mississippi Sound near Merrill Shell, and was observed to be highest at location E. These results demonstrate that levels of TP Unfilt varied between the vEFDC and SWAT-vEFDC models.

3.3. Sensitivity Analysis

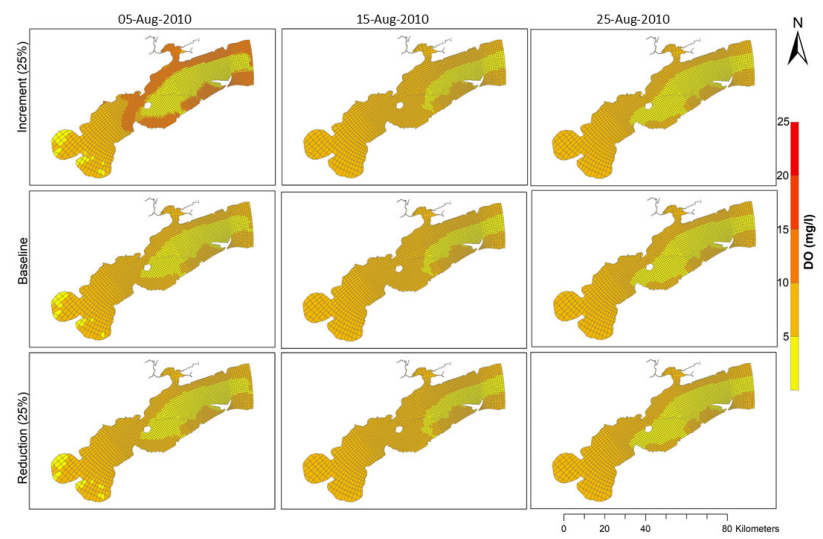
The impact of changing riverine inflow nutrient concentrations on water quality within the WMSS was studied during an extreme weather event. Various water quality parameters from the Jourdan River and the Wolf River inflows were adjusted. A 25% increase and 25% decrease in RPOP, LPOP, DOP, PO_4 , RPON, LPON, DON, NH_4 , and $NO_2 + NO_3$ were made one at a time in the model to perform the nutrient sensitivity analysis [39]. From 10 to 18 August 2010, a tropical depression named Five 2010 (<https://oceanservice.noaa.gov/news/historical-hurricanes/>) (accessed on 3 August 2023) passed through the watershed area. Therefore, 5 August, 15 August, and 25 August were selected as the representative dates on which to observe the changes in nutrition distribution throughout the grid in order to account for 25% increase, baseline, and 25% decrease scenarios. In Figure 8a–e, the changes in water quality concentration during the tropical depression are shown for DO, TN Filt, TP Filt, TN Unfilt, and TP Unfilt at selected locations in the WMSS.

The impact of nutrient concentration changes on DO levels throughout the selected locations in the WMSS during the tropical depression is shown in Figure 8a. Before the tropical depression, in the scenario with a 25% nutrient load increase, the DO level was high closer to the freshwater inflow area, the adjacent SLB area, and the area towards the end of the WMSS grid. The DO level was observed reducing with the occurrence of the tropical depression. After the tropical depression was over, the number of grids with lower DO levels increased in the midsection of the WMSS. Nutrient variation shows notable change in the 25% increment scenario before the tropical depression, whereas notable variation in DO level in the inflow from the JRW and the WRW was not observed in the nutrient load reduction scenario throughout the WMSS grid. All the images in Figure 8a show that the DO level was higher at the boundary and lower in the inside section of the WMSS grid.

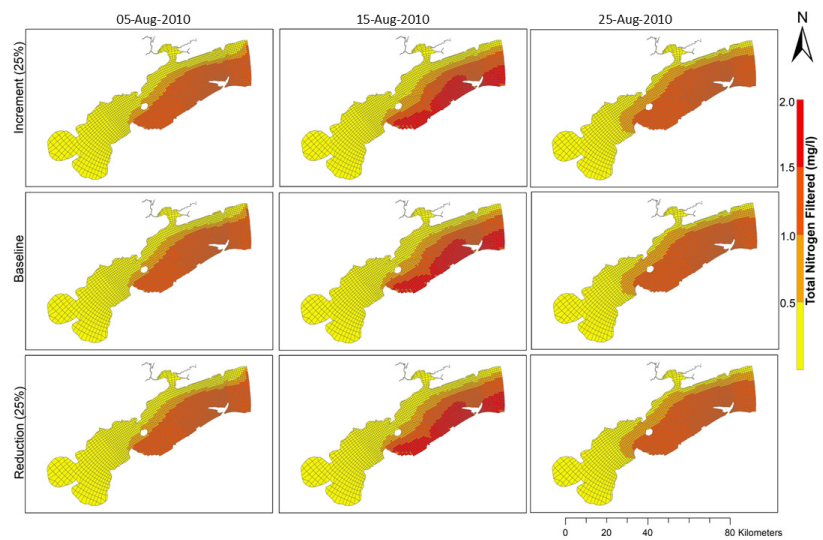
Figure 8b shows TN Filt sensitivity analysis due to the nutrient load variation during the tropical depression throughout the WMSS. Notable effects of the nutrient load variation were not observed near the inflow zone and throughout the WMSS grid. The major impact due to the tropical depression was detected as represented by a higher concentration of TN Filt in Figure 8b, and its impact was observed prevailing through 25 August.

Similarly, in Figure 8c, the impact of nutrient load variation from a freshwater inflow in TP Filt concentration during the tropical depression throughout the WMSS is presented. Notable effects of nutrient load variation were not seen near the inflow zone and throughout the WMSS; a rather more notable impact was observed because of the extreme weather. Higher concentrations of TP Filt were observed before and after the tropical depression, and a decrease in the concentration of TP Filt was observed during the tropical depression. The reason for this could be a tropical depression-induced flash flood draining a larger volume of freshwater into the WMSS.

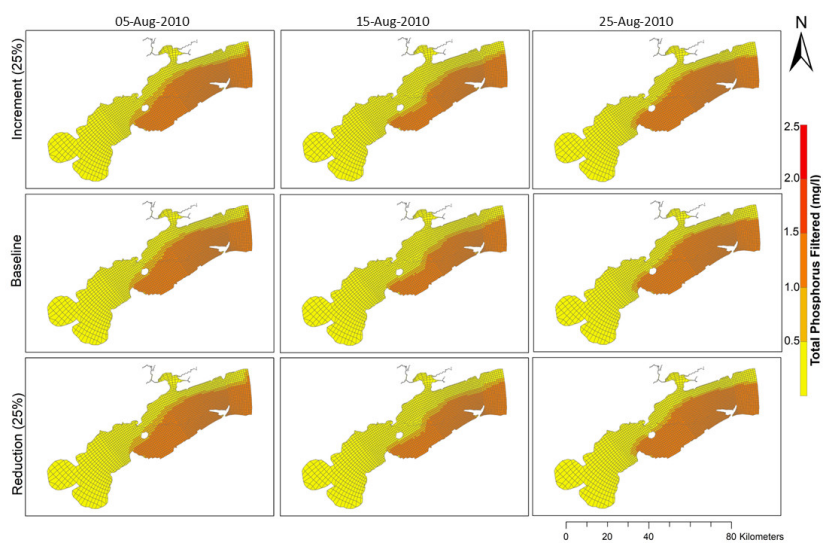
Figure 8d represents the TN Unfilt sensitivity analysis due to the nutrient load variation in the freshwater during Five throughout the WMSS. Before the tropical depression, freshwater inflow did not show notable variations in TN Unfilt concentration near the inflow zone. However, during the tropical depression, more influence from the coastal water was observed in the WMSS reaching SLB. The TN Unfilt concentration at the WRW inflow zone was observed more in the baseline and 25% increase nutrient load scenarios, surpassing the 25% reduced nutrient load scenario. An aftereffect of Five was observed in the post-tropical depression scenario, where TN Unfilt concentration was higher in all nutrient load scenarios.



(a)



(b)



(c)

Figure 8. Cont.

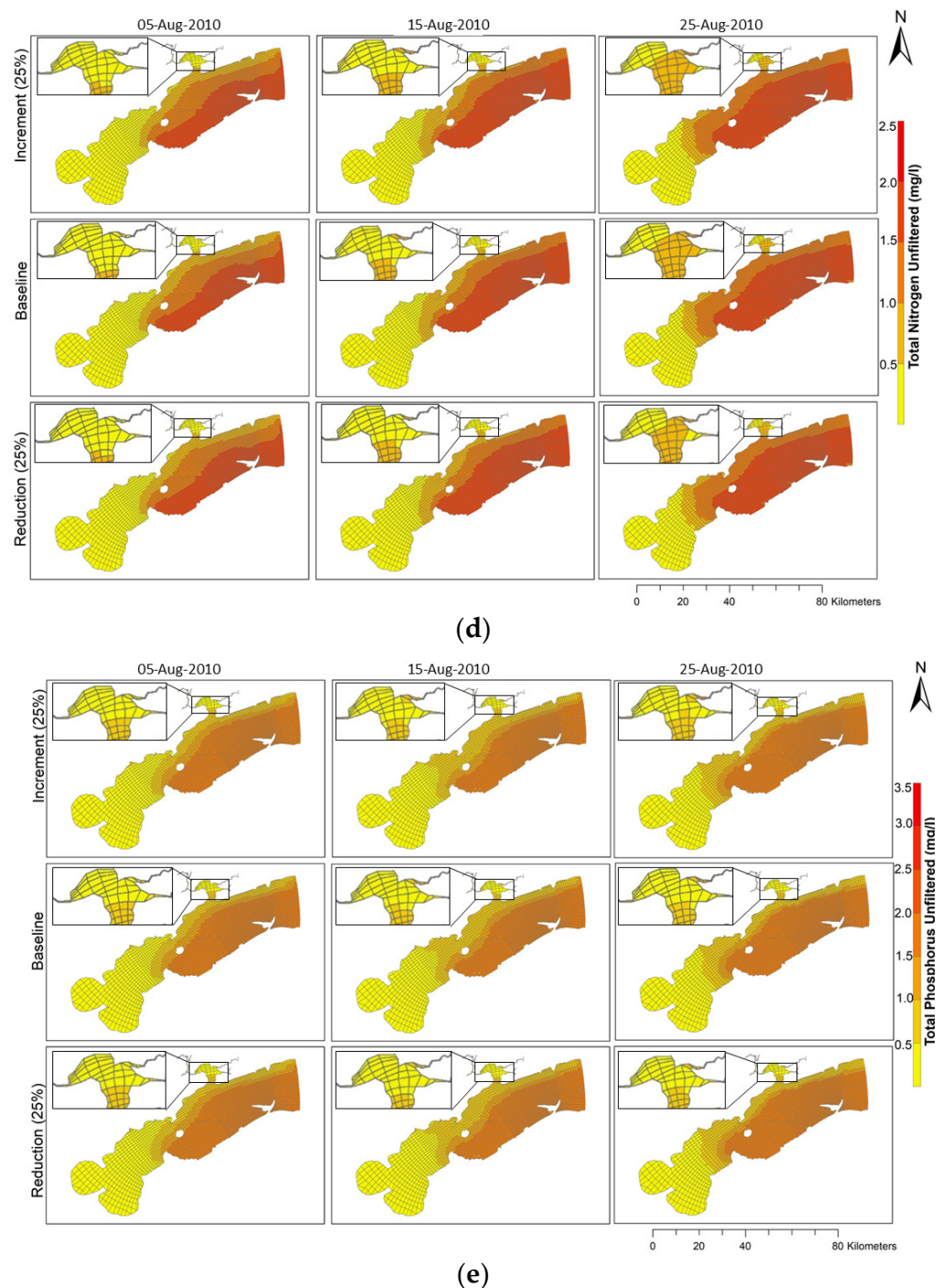


Figure 8. (a) Sensitivity analysis of nutrient load variation in DO level throughout the WMSS grid. (b) Sensitivity analysis of nutrient load variation in total nitrogen filtered concentration throughout the WMSS grid. (c) Sensitivity analysis of nutrient load variation in total phosphorus filtered concentration throughout the WMSS grid. (d) Sensitivity analysis of nutrient load variation in total nitrogen unfiltered concentration throughout the WMSS grid. (e) Sensitivity analysis of nutrient load variation in total phosphorus unfiltered concentration throughout the WMSS grid.

Similarly, Figure 8e shows the sensitivity analysis of nutrient load variation on TP Unfilt concentration during the tropical depression, throughout the WMSS grid. An extended impact on TP Unfilt concentration was seen reaching SLB in all scenarios. The image shows that during and after the occurrence of Five, the concentration of TP Unfilt

increased at the WRW inflow zone as compared to that before the tropical depression in all nutrient load scenarios.

4. Discussion

In this study, the concept of coupling hydrological and hydrodynamical models for a better understanding of hydrodynamical processes in the WMSS has been demonstrated. Graphical comparisons of flow simulated by the SWAT model and that obtained through the weighted-area model showed similar trends, where the weighted-area flow showed higher peaks and the statistical metrics demonstrated goodness of fit. In addition, the introduction of freshwater simulated by the coupled model showed a substantial change in the water quality parameters. A pronounced impact on TN and TP was observed at the point where freshwater from the Wolf River and the Jourdan River flows into the bay. This effect decreased towards the end of bay and further diminished as the water moved away from the bay. The weakening effect was due to the increasing mixture of freshwater in the coastal water. Ultimately, the impact of the freshwater was greatly reduced by the time it reached the Western Mississippi Sound. Nutrient sensitivity analysis during extreme weather conditions demonstrated that a 25% variation in the nutrient load of freshwater inflow had lower influence in the water quality of the WMSS in comparison to the influence of wind and storm surges during a tropical depression.

The results of this study are consistent with previous studies which assessed water quality by coupling the hydrodynamics model with the hydrological model. Hwang et al. [10] evaluated different water quality improvement scenarios in an estuarine reservoir, with a levee in middle, which was affected by point and non-point source pollution from the upstream basin and thus concluded that SWAT-EFDC coupling could improve water quality results. Wu et al. [13] stated that the combination of the SWAT and EFDC models addressed the limitations in measured data of upstream watersheds, and it was feasible to identify the association between sources of pollution and water quality response. Kim et al. [12] developed a watershed–estuary linkage model with the HSPF-EFDC-WASP tool to assess the impact of the drainage gate operation on water quality in the Ganwol Reservoir, Korea. The study reported that the outcome of the simulations for different water quality parameters across various locations of the reservoir was different and a pronounced effect was observed at the location near to the drainage gate operation, the inlet point [12], similar to the findings of our study. Additionally, Shin et al. [40] demonstrated the influence of wind during hurricane events in the variation of water quality parameters at Lake Okeechobee, corresponding to the outcomes of our analysis.

This study assessed the water quality at five different locations of SLB and observed variations in the effects of freshwater inflow. This study also highlights the diminishing effect of freshwater inflow when the nutrient parameters were observed further along the coastal water body. The study attempted to fill the gap in previous hydrodynamical modelling assessments of the Western Mississippi Sound by using hydrologically simulated flow data instead of using area-weighted flow data from an adjacent watershed in the hydrodynamical model. The results of this model-coupling approach are consistent with previous studies at different sites around the globe, which were able to discuss the relationship between the spatial variation of water quality parameters within coastal waters.

5. Conclusions

This study focused on the coupling of two watershed-scale SWAT models developed for the Wolf River and the Jourdan River with the vEFDC model of the estuary and bay linking the Western Mississippi Sound to make an integrated river–bay–estuary model. The calibrated/validated streamflow and nutrients data from the hydrological and water quality SWAT model were provided as an input to the calibrated/validated hydrodynamic vEFDC model to understand the execution performance of the hydrodynamic model with area-weighted flow and hydrologically simulated flow. The trend of area-weighted flow and hydrological-model simulated flow was studied. Additionally, the impact of freshwater

inflow on the water of Saint Louis Bay and the Western Mississippi Sound was also assessed along with the impact of nutrient load variation and extreme weather. Evaluation of salinity, dissolved oxygen, total nitrogen, and total phosphorus at various locations in Saint Louis Bay and the Western Mississippi Sound was conducted with the results obtained from the vEFDC and SWAT-vEFDC model simulations. After comparing the concentrations of water quality parameters obtained from the vEFDC and SWAT-vEFDC models, this study revealed that the freshwater inflow had a substantial impact on the levels of TN and TP in the bay, which gradually decreased as the water diluted when moving further along into the Western Mississippi Sound. Nutrient sensitivity analysis during the tropical depression demonstrated that a 25% variation in the nutrient load inflow contributed less than the influence of wind and storm surges in changing the water quality. In conclusion, coupling hydrological models with hydrodynamical models can be useful in assessing the impact of freshwater inflows into estuarine systems. The SWAT-vEFDC coupled approach thus provided insight into the variations in the calculated and simulated flow and water quality parameters. This study also provides insights into approaches to assessing the impact of freshwater inflows into coastal waters, understanding the model coupling method to couple a watershed model and a receiving water model can develop an integrated river–bay–estuary modelling system which can aid in integrated coastal management.

In conclusion, this study provides an insight into water quality management and aquatic ecosystem response during hurricanes. The results can be helpful in the prediction of nutrient surges in ecosystems due to runoff during extreme weather. Sediment and nutrient loading can be minimized from the coastal watershed into estuaries, wetlands, and bays by scientific result-driven policies. Moreover, habitat restoration efforts can be optimized which in turn will aid the economy of the state of Mississippi. The interaction between storm surges, watershed runoff, and sediment–nutrient transport and extreme weather conditions helps support coastal planning and emergence preparedness, and enhances understanding of ecosystem resiliency and extreme event impacts on coastal areas. This dynamic modelling approach will eventually aid in integrated coastal zone management, formulating long-term adaptation strategies to mitigate extreme weather. This study improves our understanding of applying models to the Wolf and Jourdan Rivers, which are two major tributaries feeding the Saint Louis Bay. However, future application of such models to other small bayous, such as Johnson, Portage, Four Dollar, and Rotten, may help to provide additional information on the hydrodynamics of the Saint Louis Bay. In addition, the availability and use of longer-time observed data for validating the model's performance might further improve model calibration and validation processes including sensitivity analysis of the model's parameters.

Author Contributions: S.B.: methodology, model development, data analysis, and writing original draft. P.P.: conceptual, supervision, funding acquisition, reviewing, and editing. A.L.: reviewing and editing. All authors have read and agreed to the published version of the manuscript.

Funding: This project was paid for in part with federal funding from the U.S. Department of the Treasury, the Mississippi Department of Environmental Quality, and the Mississippi-Based RESTORE Act Center of Excellence under the Resources and Ecosystems Sustainability, Tourist Opportunities, and Revived Economies of the Gulf Coast States Act of 2012 (RESTORE Act). The statements, findings, conclusions, and recommendations are those of the authors and do not necessarily reflect the views of the Department of the Treasury, the Mississippi Department of Environmental Quality, or the Mississippi-Based RESTORE Act Center of Excellence. We would like to acknowledge the partial support from the Bagley College of Engineering, Mississippi State University.

Data Availability Statement: The original contributions presented in the study are included in the article, further inquiries can be directed to the corresponding author.

Acknowledgments: We would like to acknowledge the partial support of the Bagley College of Engineering, Mississippi Agricultural and Forestry Experiment Services (MAFES), and the College of Agriculture and Life Sciences at Mississippi State University, the United States Geological Survey (USGS), and all our collaborators in this study.

Conflicts of Interest: The authors declare that they do not have any possible financial interests or personal relationships that could have influenced the work. No conflicts of interest are declared by the authors.

References

- Jordan, S.J.; Benson, W.H. Introduction Sustainable Watersheds: Integrating Ecosystem Services and Public Health Supplementary Issue: Ecosystem Services and Environmental Health. *Environ. Health Insights* **2015**, *9*, EHI-S19586. [[CrossRef](#)]
- Meshesha, T.W.; Wang, J.; Melaku, N.D. Modelling Spatiotemporal Patterns of Water Quality and Its Impacts on Aquatic Ecosystem in the Cold Climate Region of Alberta, Canada. *J. Hydrol.* **2020**, *587*, 124952. [[CrossRef](#)]
- Prasad, M.B.K.; Long, W.; Zhang, X.; Wood, R.J.; Murtugudde, R. Predicting Dissolved Oxygen in the Chesapeake Bay: Applications and Implications. *Aquat. Sci.* **2011**, *73*, 437–451. [[CrossRef](#)]
- Bhusal, A.; Ghimire, A.B.; Thakur, B.; Kalra, A. Evaluating the Hydrological Performance of Integrating PCSWMM and NEXRAD Precipitation Product at Different Spatial Scales of Watersheds. *Model. Earth Syst. Env.* **2023**, *9*, 4251–4264. [[CrossRef](#)]
- Fabian, P.S.; Kwon, H.-H.; Vithanage, M.; Lee, J.-H. Modeling, Challenges, and Strategies for Understanding Impacts of Climate Extremes (Droughts and Floods) on Water Quality in Asia: A Review. *Env. Res.* **2023**, *225*, 115617. [[CrossRef](#)]
- Flipo, N.; Gallois, N.; Schuite, J. Regional Coupled Surface–Subsurface Hydrological Model Fitting Based on a Spatially Distributed Minimalist Reduction of Frequency Domain Discharge Data. *Geosci. Model. Dev.* **2023**, *16*, 353–381. [[CrossRef](#)]
- Parajuli, U.; Bhusal, A.; Babu Ghimire, A.; Shin, S. Comparing HEC-HMS, PCSWMM, and Random Forest Models for Rainfall-Runoff Evaluation to Extreme Flooding Events. In Proceedings of the World Environmental and Water Resources Congress 2023: Adaptive Planning and Design in an Age of Risk and Uncertainty—Selected Papers from World Environmental and Water Resources Congress, Henderson, NV, USA, 21–24 May 2023; pp. 1250–1262. [[CrossRef](#)]
- Sun, G.; Wei, X.; Hao, L.; Sanchis, M.G.; Hou, Y.; Yousefpour, R.; Tang, R.; Zhang, Z. Forest Hydrology Modeling Tools for Watershed Management: A Review. *Ecol. Manag.* **2023**, *530*, 120755. [[CrossRef](#)]
- Tarpanelli, A.; Paris, A.; Sichangi, A.W.; O’Loughlin, F.; Papa, F. Water Resources in Africa: The Role of Earth Observation Data and Hydrodynamic Modeling to Derive River Discharge. *Surv. Geophys.* **2022**, *44*, 97–122. [[CrossRef](#)]
- Hwang, S.; Jun, S.M.; Song, J.H.; Kim, K.; Kim, H.; Kang, M.S. Application of the SWAT-EFDC Linkage Model for Assessing Water Quality Management in an Estuarine Reservoir Separated by Levees. *Appl. Sci.* **2021**, *11*, 3911. [[CrossRef](#)]
- Hwang, S.; Jun, S.M.; Kim, K.; Kim, S.H.; Lee, H.; Kwak, J.; Kang, M.S. Development of a Framework for Evaluating Water Quality in Estuarine Reservoir Based on a Resilience Analysis Method. *J. Korean Soc. Agric. Eng.* **2020**, *62*, 105–119. [[CrossRef](#)]
- Kim, S.; Kim, S.; Hwang, S.; Lee, H.; Kwak, J.; Song, J.H.; Jun, S.M.; Kang, M.S. Impact Assessment of Water-Level Management on Water Quality in an Estuary Reservoir Using a Watershed-Reservoir Linkage Model. *Agric. Water Manag.* **2023**, *280*, 108234. [[CrossRef](#)]
- Wu, L.; Chen, Z.; Ding, X.; Liu, H.Y.; Wang, D.Q. Research on Water Environmental Capacity Accounting of the Yongzhou Section of Xiangjiang River Basin Based on the SWAT-EFDC Coupling Model. *J. Water Clim. Chang.* **2022**, *13*, 1106–1122. [[CrossRef](#)]
- Zhang, C.; Huang, Y.; Javed, A.; Arhonditsis, G.B. An Ensemble Modeling Framework to Study the Effects of Climate Change on the Trophic State of Shallow Reservoirs. *Sci. Total Environ.* **2019**, *697*, 134078. [[CrossRef](#)] [[PubMed](#)]
- Neitsch, S.L.; Arnold, J.G.; Kiniry, J.R.; Srinivasan, R.; Williams, J.R. SWAT2000 User’s Manual VERSION 2000. 2005. Available online: <https://www.scribd.com/document/145722143/SWAT2000-User-s-Manual> (accessed on 7 March 2023).
- Tetra Tech Inc. *The Environmental Fluid Dynamics Code User Manual US EPA*, Version 1.01; Tetra Tech Inc.: Fairfax, VA, USA, 2007.
- Tetra Tech Inc. *The Environmental Fluid Dynamics Code Theory and Computation Volume 3: Water Quality Module*; Tetra Tech Inc.: Fairfax, VA, USA, 2007; Volume 2, p. 96.
- Mississippi Commission on Environmental Quality. *Regulations for Surface Water Quality Criteria for Intrastate, Interstate, and Coastal Waters*; MDEQ: Jackson, MI, USA, 2021; pp. 39289–40385.
- Armandei, M.; Linhoss, A.C.; Camacho, R.A. Hydrodynamic Modeling of the Western Mississippi Sound Using a Linked Model System. *Reg. Stud. Mar. Sci.* **2021**, *44*, 101685. [[CrossRef](#)]
- Tetra Tech Inc. *Visual EFDC 2.0 User’s Guide, A Grid Generation, Editing, Pre- and Post-Processing Tool for EFDC Hydrodynamic and Water Quality Modeling 2018*; Tetra Tech Inc.: Fairfax, VA, USA, 2018.
- Bazgirkhoob, H.; Linhoss, A.; Armandei, M. A Numerical Tool for Dissolved Oxygen Simulation in the Western Mississippi Sound. *J. Coast. Res.* **2022**, *38*, 699–711. [[CrossRef](#)]
- Bhattacharai, S.; Parajuli, P.B. Best Management Practices Affect Water Quality in Coastal Watersheds. *Sustainability* **2023**, *15*, 4045. [[CrossRef](#)]
- Arnold, J.G.; Srinivasan, R.; Muttiah, R.S.; Williams, J.R. Large Area Hydrologic Modeling and Assessment Part 1: Model Development. *J. Am. Water Resour. Assoc.* **1998**, *34*, 73–89. [[CrossRef](#)]
- Wang, Y.; Jiang, R.; Xie, J.; Zhao, Y.; Yan, D.; Yang, S. Soil and Water Assessment Tool (SWAT) Model: A Systemic Review. *J. Coast. Res.* **2019**, *93*, 22–30. [[CrossRef](#)]
- Bhattacharai, S.; Parajuli, P.B.; To, F. Comparison of Flood Frequency at Different Climatic Scenarios in Forested Coastal Watersheds. *Climate* **2023**, *11*, 41. [[CrossRef](#)]
- Venishetty, V.; Parajuli, P.B.; To, F. Assessing the Effect of Spatial Variation in Soils on Sediment Loads in Yazoo River Watershed. *Hydrology* **2023**, *10*, 62. [[CrossRef](#)]

27. Venishetty, V.; Parajuli, P.B. Assessment of BMPs by Estimating Hydrologic and Water Quality Outputs Using SWAT in Yazoo River Watershed. *Agriculture* **2022**, *12*, 477. [[CrossRef](#)]
28. Francesconi, W.; Srinivasan, R.; Pérez-Miñana, E.; Willcock, S.P.; Quintero, M. Using the Soil and Water Assessment Tool (SWAT) to Model Ecosystem Services: A Systematic Review. *J. Hydrol.* **2016**, *535*, 625–636. [[CrossRef](#)]
29. Liu, M.; Chen, X.; Yao, H.; Chen, Y. A Coupled Modeling Approach to Evaluate Nitrogen Retention within the Shanmei Reservoir Watershed, China. *Estuar. Coast. Shelf Sci.* **2015**, *166*, 189–198. [[CrossRef](#)]
30. Parajuli, P.B.; Risal, A. Evaluation of Climate Change on Streamflow, Sediment, and Nutrient Load at Watershed Scale. *Climate* **2021**, *9*, 165. [[CrossRef](#)]
31. Abbaspour, K.C. *SWAT-CUP 2012: SWAT Calibration and Uncertainty Programs—A User Manual*; Eawag: Dübendorf, Switzerland, 2014; Volume 106.
32. Saline Water and Salinity | U.S. Geological Survey. Available online: <https://www.usgs.gov/special-topics/water-science-school/science/saline-water-and-salinity> (accessed on 7 March 2023).
33. Tang, X.; Xie, G.; Deng, J.; Shao, K.; Hu, Y.; He, J.; Zhang, J.; Gao, G. Effects of Climate Change and Anthropogenic Activities on Lake Environmental Dynamics: A Case Study in Lake Bosten Catchment, NW China. *J. Env. Manag.* **2022**, *319*, 115764. [[CrossRef](#)]
34. Telesh, I.V.; Khlebovich, V.V. Principal Processes within the Estuarine Salinity Gradient: A Review. *Mar. Pollut. Bull.* **2010**, *61*, 149–155. [[CrossRef](#)]
35. Kang, M.; Peng, S.; Tian, Y.; Zhang, H. Effects of Dissolved Oxygen and Nutrient Loading on Phosphorus Fluxes at the Sediment–Water Interface in the Hai River Estuary, China. *Mar. Pollut. Bull.* **2018**, *130*, 132–139. [[CrossRef](#)]
36. Zhou, J.; Han, X.; Brookes, J.D.; Qin, B. High Probability of Nitrogen and Phosphorus Co-Limitation Occurring in Eutrophic Lakes. *Environ. Pollut.* **2022**, *292*, 118276. [[CrossRef](#)]
37. Park, J.; Kim, K.T.; Lee, W.H. Recent Advances in Information and Communications Technology (ICT) and Sensor Technology for Monitoring Water Quality. *Water* **2020**, *12*, 510. [[CrossRef](#)]
38. Moriasi, D.N.; Gitau, M.W.; Pai, N.; Daggupati, P.; Gitau, M.W.; Member, A.; Moriasi, D.N. Hydrologic and Water Quality Models: Performance Measures and Evaluation Criteria. *Trans. ASABE* **2015**, *58*, 1763–1785. [[CrossRef](#)]
39. Luo, C.; Li, Z.; Wu, M.; Jiang, K.; Chen, X.; Li, H. Comprehensive Study on Parameter Sensitivity for Flow and Nutrient Modeling in the Hydrological Simulation Program Fortran Model. *Environ. Sci. Pollut. Res.* **2017**, *24*, 20982–20994. [[CrossRef](#)] [[PubMed](#)]
40. Shin, S.; Her, Y.; Muñoz-Carpena, R.; Yu, X. Quantifying the Contribution of External Loadings and Internal Hydrodynamic Processes to the Water Quality of Lake Okeechobee. *Sci. Total Environ.* **2023**, *883*, 163713. [[CrossRef](#)] [[PubMed](#)]

Disclaimer/Publisher’s Note: The statements, opinions and data contained in all publications are solely those of the individual author(s) and contributor(s) and not of MDPI and/or the editor(s). MDPI and/or the editor(s) disclaim responsibility for any injury to people or property resulting from any ideas, methods, instructions or products referred to in the content.